A DISSERTATION ON

"Synthesis and Characterization of MnS Nanoparticles"

Submitted To The
Department Of Physics
Faculty Of Science
Integral University, Lucknow

IN PARTIAL FULFILMENT
FOR THE
DEGREE OF MASTER OF SCIENCE
IN PHYSICS

BY,
Humaira Ansari
M.Sc. Physics (IV Semester)
Roll No: 2101080003

UNDER THE SUPERVISION OF,

Ms. Tahira Khatoon,
Department of Physics
INTEGRAL UNIVERSITY
LUCKNOW-226026, UP INDIA

INTEGRAL UNIVERSITY

Established Under the Integral University Act 2004 (U.P. Act No.9 of 2004)
Approved by University Grant Commission under Sections 2(f) and 12B
Phone No.: +91(0522) 2890812, 2890730, 3296117, 6451039, Fax No.: 0522-2890809
Kursi Road, Lucknow-226026 Uttar Pradesh (INDIA)

CERTIFICATE BY SUPERVISOR

This is to certify that, **Humaira Ansari**, a student of M. Sc. (Physics-IV Semester) has successfully completed the dissertation on "**Synthesis and Characterization of MnS Nanoparticles**" under my supervision during the year 2022-2023. It is certified that the work has not been submitted anywhere else for the award of any other diploma or degree of this or any other University.

I wish her good luck and bright future.

Date:10 June 2021
Place: Lucknow

Ms TAHIRA KHATOON
Supervisor
Assistant Professor (Level II)
Department of Physics
Integral University,
Lucknow-226026

INTEGRAL UNIVERSITY

Established Under the Integral University Act 2004 (U.P. Act No.9 of 2004)
Approved by University Grant Commission under Sections 2(f) and 12B
Phone No.: +91(0522) 2890812, 2890730, 3296117, 6451039, Fax No.: 0522-2890809
Kursi Road, Lucknow-226026 Uttar Pradesh (INDIA)

CERTIFICATE BY HOD

This is to certify that **Humaira Ansari** is a student of M. Sc. (Physics-IV Semester) Session 2021- 22 to 2022-23 at Integral University, Lucknow. She completed her project entitled **"Synthesis and Characterization of MnS Nanoparticles"** successfully under the supervision of Ms. Tahira Khatoon, Assistant Professor (Level II), Department of Physics, Integral University.

I wish her good luck and bright future.

Date:10 June 2023
Place: Lucknow

(Dr. Seema Srivastava)
Head
Department of Physics
Integral University
Lucknow-226026

ACKNOWLEDGMENT

I find it difficult to suitably express my deepest sense of gratitude to almighty for the completion of my dissertation project work in time.

This dissertation work is dedicated to those who gave me an opportunity and encouragement to inculcate fineness in report.

I would like to express my sincere gratitude towards all the people who have contributed their precious time and effort to help me, without them it would have been a great difficulty for me to understand and complete the project.

I would especially like to thank Ms. Tahira Khatoon Ma'am, Assistant Professor (Level II), Department of Physics, my supervisor for her guidance, support, motivation, and encouragement throughout the period this work was carried out. Her readiness for consultation always, her educative comments, her concern, and assistance even with practical things have been invaluable.

I am grateful to Dr. Seema Srivastava, Associate Professor and Head, Department of Physics for providing necessary facilities in the department.

Last but not the least I would like to offer my gratitude and my special thanks to all the members and students of my Department of Physics, Integral University for their kind help. It continues to my family members, my well-wishers and friends who encouraged me to precede the work sincerely and seriously.

My heartiest thank goes to all the above for helping me a lot to build up a fruitful project work.

Humaira. Ansari

HUMAIRA ANSARI

Contents

List of Figures

List of Abbreviations

MnS   Manganese Sulfide

PVP   Polyvinylpyrrolidone

MRI   Magnetic Resonance Imaging

CNT   Carbon Nanotubes

SWCNT   Single Walled Carbon Nanotubes

MWCNT   Multi Walled Carbon Nanotube

CVD   Chemical Vapor Deposition

FCC   Face Centered Cubic

XRD   X-Ray Diffraction

SEM   Scanning Electron Microscope

UV-DRS   Ultraviolet Diffraction Reflectance Spectroscopy

FTIR   Fourier Transformation Infrared Spectroscopy

BSE   Backscattered Electrons

ABSTRACT

For both fundamental and applied research, manganese(II) sulfide (MnS) is an intriguing substance, particularly when its bulk characteristics are altered by shrinking the size into the nanometric zone (100 nm). MnS is a desirable material to create synthetic techniques for polymorphism control because of its polymorphism. We looked over the research on MnS nanomaterials with at least one dimension under 100 nm. With an emphasis on solvothermal techniques and studies devoted to understanding the growth mechanism and the polymorphism, effective synthetic techniques are presented for the preparation of zero- and one-dimensional MnS nanomaterials (either homogeneous or heterogeneous) with control over size, shape, and polymorphism. The characteristics and uses of nanosize MnS employed as optical, electric, and magnetic materials are grouped into three major categories. MnS is attractive because of its wide bandgap, which makes it promising for UV emission. Since MnS is antiferromagnetic at low temperatures and (super)paramagnetic at moderate temperatures, its magnetic characteristics have also attracted interest. Finally, since the insertion and exchange of tiny ions is made simple by the layered structure of the hexagonal polymorph, nanosize MnS performs well as a lithium-ion battery electrode or supercapacitor material. We can regulate the precise crystal phase of the product by adjusting the injection temperature and subsequent ageing period. There are three known polymorphs of MnS, and two of them are R-MnS.

1.INTRODUCTION

1.1 Introduction to Nanomaterials

As the name implies, nanomaterials are substances with dimensions between 1 to 100 nanometers, or at the nanoscale level. At this scale, materials display distinctive characteristics and actions that set them apart from their bulk counterparts. The field of nanomaterials has gained significant attention in recent years due to its potential for revolutionizing various industries, including electronics, medicine, energy, and environmental applications. This introduction aims to provide an overview of nanomaterials, their properties, synthesis methods, and potential applications(1).

The high surface area-to-volume ratio of nanoparticles is one of their distinguishing characteristics. As materials are reduced to the nanoscale, a higher proportion of their atoms or molecules resides on the surface compared to the interior. This increased surface area gives rise to enhanced reactivity, making nanomaterials ideal for catalytic applications. Additionally, nanomaterials exhibit size-dependent properties, meaning that their physical, chemical, and optical characteristics can significantly change as their size decreases.

A multidisciplinary discipline of science and engineering called nanotechnology has emerged as a revolutionary force that has the potential to drastically alter many facets of our existence. Nanotechnology enables the development of materials, tools, and systems with improved characteristics and functions by modifying matter at the atomic and molecular levels. Scientists, engineers, and researchers from all around the world are fascinated by this developing discipline because it presents unheard-of chances to address pressing issues in numerous industries. In this introduction, we will examine the underlying ideas, uses, and consequences of nanotechnology, emphasizing its potential for change and the important fields it affects.

1.2 Manganese Sulfide

Under ambient temperature (Eg = 3 eV), manganese (II) sulfide (MnS), a p-type semiconductor, transforms into an antiferromagnetically ordered phase. The potential applications of nanosized MnS in the fields of short-wavelength optoelectronics, or as a photoluminescent component, photoreduction catalysts, or contras tent for magnetic resonance imaging (MRI), were made interesting by

these features. Recently, intriguing energy-related applications have been proven, using MnS as a supercapacitor material and an electrode material in Li-ion batteries(2).

Alabandite (R-MnS), a naturally occurring form of manganese sulfide (MnS), has been the focus of current photoelectrochemical research to investigate the possibility that MnS contributed to prebiotic synthesis on the early Earth.1 The use of crystalline MnS produced without the addition of any organosulfur compounds avoids the need to add further carbon sources in these photochemical investigations. In this paper, we describe an organosulfur-free aqueous method to producing pure R-MnS (3). Our results are in line with earlier research, which is mentioned below, which showed that reaction temperature and ageing time had a significant impact on the abundance of the different MnS phases precipitated by solvothermal techniques. In this paper, we describe an organosulfur-free aqueous method to producing pure R-MnS. Our results are in line with earlier research, which is mentioned below, which showed that reaction temperature and ageing time had a significant impact on the abundance of the different MnS phases precipitated by solvothermal techniques. At normal temperature, the kinetic generation of the thermodynamically stable R-phase is prevented; nevertheless, under solvothermal circumstances, this phase will develop easily at temperatures above 200 °C (4).

Three polymorphs of MnS can crystallize, and each has unique structural and physical characteristics. In numerous other experimental works, R-MnS was produced from inorganic precursors that were first converted to MnS under aqueous circumstances before being dried. Using heating at a high temperature (1000 °C). Prior research has also documented the use of solvothermal synthesis methods to produce stable (R) MnS as well as metastable polymorphs (5). To the best of our knowledge, all of the earlier research involved the synthesis of MnS depended either on the use of elemental components or on the thermal breakdown of an organic precursor at a high temperature in conjunction with a lengthy ageing period. In particular, â-MnS were previously found to develop solely in nonaqueous circumstances (6). The -phase and this phase's free energy of production among the MnS polytypes are closely related. Lu et al.17 were successful in creating â-MnS in a tetrahydrofurane ether solvent and -MnS in

benzene hydrocarbon solvent. The two solvents employed in this instance were nonpolar and nonaqueous. This result suggests that the precipitation kinetics within the Mn-S system are significantly influenced by the solvent's polarity and relatively little differences in the surface tensions of the three polymorphs. Two far more recent MnS crystals have been reported on: bowenite (-MnS), which was found in a meteorite recovered in Poland in 2012, and rambergite (-MnS), which was identified in Sweden in 1996 (7).

Our review is restricted to pure MnS nanostructures with at least one dimension smaller than 100 nm that are homogeneous or heterogeneous (certain MnS sub-microcrystals are included when of exceptional interest). One-dimensional (1D) and zero-dimensional (0D) MnS nanomaterials have both been created utilizing a variety of bottom-up techniques, including chemical vapor deposition (CVD) hydrothermal "wet" methods. On the other hand, 1D nanomaterials (rods, wires, and saws) were frequently created using the CVD method. Additionally, several solvothermal or CVD procedures have been used to create heterostructures using MnS that are both 0D and 1D and exhibit unique features(8). Controlling polymorphism in 0D NCs is a problem has been the focus of numerous publications demonstrating that the desired crystal structure can be achieved using both physical and chemical parameters.

1.3 Types of Nanomaterials

Nanomaterials are substances with distinctive features and structures at the nanoscale level, usually between 1 and 100 nanometers. They can be divided into a number of categories according to their makeup, structure, and characteristics. The following list of typical nanomaterials:

Small, nanoscale-sized particles are referred to as nanoparticles. They can be created from a diversity of substances, along with metals (such as gold, silver), metal oxides (such as titanium dioxide, zinc oxide), semiconductor nanocrystals known as quantum dots, and carbon-based substances (example nanotubes of carbon and fullerenes).

Nanowires are elongated, thin structures with lengths often greater than the diameter and diameters in the nanoscale range. Materials such as metals, semiconductors, and insulators can all be used to create nanowires.

Carbon nanotubes (CNTs) are cylinder-shaped materials that are entirely composed of carbon atoms. Single-walled carbon nanotubes or multi-walled carbon nanotubes (SWCNTs or MWCNTs) are two possible types. The strength, thermal conductivity, and electrical conductivity of carbon nanotubes are remarkable.

Materials called nanocomposites are made of a matrix material and nanoparticles or nanofibers. To improve the overall qualities of the composite material, the nanoparticles or nanofibers are disseminated throughout the matrix. For instance, introducing carbon nanotubes to polymers can increase their electrical conductivity and mechanical strength.

Nanolayers are extremely thin layers of substance that typically have a thickness of a few nanometers to several hundred nanometers. Using methods like chemical vapor deposition or physical vapor deposition, nanolayers can be deposited on substrates. They are used in many different applications, such as electronic devices, coatings, and sensors.

Materials containing a network of tiny pores or cavities are referred to as nanoporous materials. They frequently have a large surface area and are suitable for filtration, gas storage, and catalysis. Examples include metal-organic frameworks (MOFs), zeolites, and nanoporous silica.

Crystals with dimensions closer to the nanoscale are known as nanocrystals. They can be made of a variety of substances, including metallic, magnetic, or semiconductor nanocrystals (quantum dots). Due to their small size and the effects of quantum mechanics, nanocrystals have special optical, electrical, and magnetic capabilities.

1.4 Crystal structure of MnS

The temperature at which manganese sulfide, or MnS, crystallises, affects its crystal structure. MnS crystallises in the face-centered cubic (FCC) rock salt structure when it is at room temperature. In this structure, there are six sulfur (S) ions around each manganese (Mn) ion and six sulfur ions around each manganese ion. The arrangement places the anions (S) in the FCC and the cations (Mn) in cube's corners.

MnS experiences a phase change when the temperature rises, changing into the beta phase crystal structure. MnS has a cubic crystal structure in the beta phase, with the sulfur and manganese atoms forming a face-centered cubic (fcc) lattice. Each manganese atom in this configuration coordinates with four sulfur atoms, and each sulfur atom is surrounded by four manganese atoms, giving a tetrahedral arrangement (9).

The crystal structure of MnS can change based on conditions like temperature, pressure, and the presence of impurities, it is crucial to note. For pure MnS, the most frequently observed structures are those of rock salt and however other variations can exist in certain circumstances.

The cubic crystal structure known as the rock salt structure has alternate locations for Mn and S atoms in a face-centered cubic (fcc) lattice in which crystallizes in manganese sulfide (MnS), a binary compound composed of manganese (Mn) and sulfur (S) atoms.

Lattice and Unit Cell Parameters: The unit cell is the fundamental unit of repetition in a crystal structure. The Mn and S atoms are positioned at the cube's corners and face centres, respectively, in the instance of MnS, where the unit cell is a cube. The cube's edge length is represented by the lattice parameter "a."

The lattice parameter of MnS is approximately 5.187 angstroms (Å) at ambient temperature. This value gives a decent approximation for the crystal structure of MnS, albeit it may change significantly depending on temperature and other variables (10).

Each sulfur atom in the MnS rock salt structure is coordinated by six manganese atoms, resulting in an octahedral arrangement. In an analogous octahedral coordination geometry, six sulfur atoms surround each manganese atom. Mn and S have the same coordination number, which is 6.

The majority of the bonds in MnS are ionic. As a transition metal, manganese transfers electrons to sulfur, forming the positively charged Mn ions (Mn^{2+}) and negatively charged S ions (S^{2-}). The stability of the lattice crystal is a outcome of the ionic bonds that exist between the Mn^{2+} and S^{2-} ions.

Rock salt's structure displays a great degree of symmetry and packing. It belongs to the face-centered cubic (fcc) lattice of the cubic crystal system. The absence of any extra symmetry components beyond those found in the fcc lattice is shown by the space group Fm-3m.

The Mn and S atoms are arranged in a tightly packed configuration. The corners of the cubic unit cell are home to the manganese atoms, while the face centres are occupied by the sulfur atoms. This configuration produces a dense crystal structure and maximizes packing efficiency. The corners of the cube and the centres of each face are where the lattice points are found in the fcc lattice. Depending on the lattice point, an atom of sulfur or manganese is represented. A stacking sequence of densely packed planes can be used to visualize the atom arrangement in the MnS crystal structure (11).

The subsequent plane is placed directly on top of the first one, with the lattice parameter's offset reduced by half. The crystal lattice is covered in a repeated pattern as a result of this stacking sequence. It is common to depict the MnS crystal structure as a three-dimensional arrangement of stacked planes.

We can look at the immediate surroundings of each atom in MnS to describe the coordination geometry of those atoms. Six manganese atoms surround each sulfur atom in MnS to provide an octahedral coordination geometry. Six sulfur atoms, also in an octahedral configuration, coordinate each manganese atom. Manganese and sulfur both have a coordination number of 6.
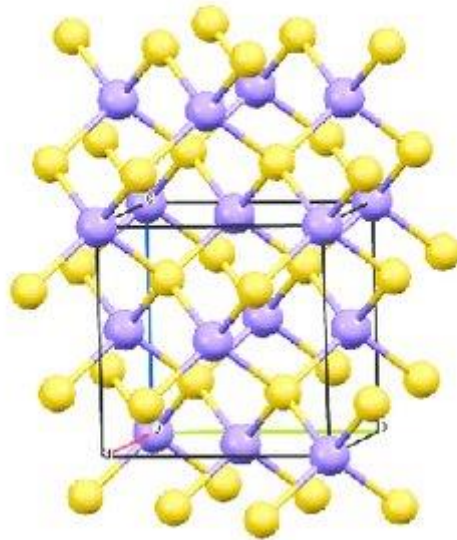
Figure 1: Crystal Structure of MnS

The closely packed arrangement of atoms in the crystal lattice results in the octahedral coordination geometry. The surrounding atoms combine to form symmetrical octahedra with the central atom (either Mn or S) at the centre. The close-packed planes stack together in a predictable way, leading to this coordination arrangement. The spacing between lattice points in the rock salt structure might change slightly with temperature and other factors, according to lattice characteristics. However, the MnS lattice parameter is roughly 5.187 angstroms at ambient temperature. The distance between consecutive lattice points in a crystal lattice is represented by this number (12).

Overall, the atomic arrangement and great symmetry of the MnS crystal structure can be described as tightly packed. The electrical conductivity, mechanical toughness, and optical behavior of MnS are all influenced by this arrangement's physical and chemical characteristics. For research into MnS's characteristics and uses, understanding its crystal structure is crucial. X-ray diffraction and electron microscopy are two methods that scientists frequently use to identify and see the crystal structure of materials. Scientists can learn more about the behaviour and characteristics of MnS in a variety of domains, including as materials science, chemistry, and solid-state physics, by looking at the positioning of atoms in the crystal lattice. There are numerous significant implications for the properties of MnS based on its crystal structure. First off, the rock salt structure has a high

density due to the way the atoms are packed together. MnS has a density of around 3.99 g/cc, which is high for a compound made up of lighter elements like manganese and sulfur (13).

1.5 Properties of Manganese Sulfide

Manganese sulfide (MnS) is an inorganic substance with a number of noteworthy characteristics. Although it is frequently found in nature as the mineral alabandite, it can also be created in a lab. Usually, MnS appears as a solid in dark grey or black.

1.5.1 Optical Properties

Since MnS is typically transparent to visible light, light can pass through it without being significantly absorbed or scattered. Its broad bandgap, which blocks the absorption of light with energies below a certain threshold, is what causes this transparency. MnS appears optically clear as a result in the visible spectrum. Depending on the wavelength of the light, MnS has a refractive index that normally falls between 2.0 and 2.5 for visible light. MnS can also have luminous characteristics, which cause it to produce light when activated by an outside energy source. It is a material of interest due to its optical properties in applications like optoelectronics, solar cells, and luminous materials (14).

1.5.2 Electrical Properties

MnS, a semiconductor, has an electrical conductivity that falls in the middle of insulators and conductors. Its band structure is what causes its electrical behaviour. Between 2 and 3 electron volts (eV) is typically the energy required for an electron in MnS to cross the bandgap from the valence band to the conduction band. Increased conductivity results from more electrons being able to bridge the bandgap when temperature rises thanks to the thermal energy. On the other hand, MnS exhibits a decreased electrical conductivity at lower temperatures. With a wide bandgap, temperature-dependent conductivity, and the capacity to be doped for specific electrical properties, MnS displays semiconducting behaviour. Its employment in technological gadgets and renewable energy applications is made possible by these qualities (15).

1.5.3 Magnetic Properties

It is significant to remember that a variety of elements, including impurities, defects, and changes to the crystal structure, can have an impact on the magnetic characteristics of MnS. These elements may have an impact on the potency and temperature dependency of the MnS magnetic.

In conclusion, the unpaired electrons in the manganese ions cause MnS to behave paramagnetically. Additionally, it has a Curie temperature at which it turns into a paramagnet. Additionally, under specific circumstances, MnS can exhibit antiferromagnetic behaviour. Applications in areas like magnetic storage devices, spintronics, and magnetic materials research require an understanding of and control of these magnetic properties (16).

1.6 Processing Methods

Two methods can be successfully used to create nanomaterials. The "Bottom Up" strategy, which produces little building pieces and assembles them into enormous buildings, is the first approach. Morphology, crystallinity, particle size, and composition are the primary regulating factors in the synthesis process. Examples include self-assembly, colloidal aggregation, laser trapping, chemical synthesis, and secondly, the "Top Down" technique, which Starting with a larger substance or structure, the top-down approach in nanotechnology gradually reduces its size and dimensions to produce tiny structures. Examples include the growth and deposition of films, lithography, etching technique, etc. The primary cause of changes in various mechanical, thermal, and other properties is a rise in the surface to volume ratio.

Three different methods can be used to create nanomaterials, including

- Liquid-phase synthesis
- Gas-phase synthesis
- Vapor-phase synthesis

1.6.1 Liquid-phase synthesis

- The following synthesis techniques are used in liquid phase synthesis:
- Co-precipitation.

- Sol-gel Processing.

- Micro-emulsions.

- Hydrothermal / Solvo-thermal Synthesis.

- Microwave Synthesis.

- Sono-chemical Synthesis.

- Template Synthesis.

1.6.2 Gas-phase Synthesis

- Material is vaporized into a background gas, and the gas is subsequently cooled to produce super saturation.

1.6.3 Methods of using solid precursors

- Inert Gas Condensation

- Pulsed Laser Ablation

- Spark Discharge Generation

- Ion Sputtering

1.7 Applications of MnS nanostructures

A lot of interest has been paid to manganese sulfide (MnS) nanostructures because of their special characteristics and prospective uses in many different industries. We shall examine a few MnS nanostructure uses, emphasizing their role in energy storage, catalysis, and medicinal uses.

MnS nanostructures have demonstrated potential in energy storage systems like lithium-ion batteries and supercapacitors. A lithium-ion battery's anode can be made of MnS nanoparticles or nanowires due to its excellent electrochemical performance and high theoretical capacity. Electrical energy can be stored and released during charge and discharge cycles thanks to the conversion reaction between MnS and lithium ions. Furthermore, the distinct MnS nanostructure can offer a large surface area, quick diffusion routes for lithium ions, and increased electrode-electrolyte interactions, resulting in higher performance (17).

MnS nanostructures have proven to be catalytic in a number of chemical processes. For instance, in fuel cells and water-splitting devices, they can effectively catalyze the oxygen reduction reaction (ORR) and hydrogen evolution process (HER). The electrochemical mechanisms involved in these reactions are

made easier by the high surface area and many active sites found in MnS nanosheets or nanoparticles. Additionally, due to their capacity to stimulate particular chemical reactions with high selectivity, MnS nanostructures have demonstrated potential as catalysts for organic transformations, such as the manufacture of fine compounds and medications (18).
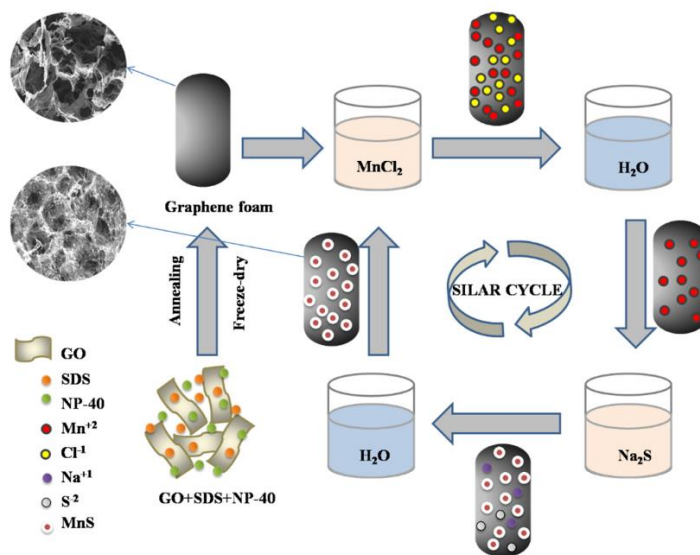
Figure 2: MnS as Catalyst

MnS nanostructures are suited for optoelectronic applications due to their optical and electrical characteristics. By varying the shape and size of the nanostructures, the bandgap of MnS can be adjusted. Their use in solar cells, photodetectors, and light-emitting diodes (LEDs) is made possible by their tunability. These devices can use MnS quantum dots or nanocrystals to emit or absorb light in particular wavelength bands. The efficiency and effectiveness of optoelectronic devices can be improved by the distinct quantum confinement phenomena seen in MnS nanostructures (19).

Magnetic resonance imaging (MRI) contrast agents, such as MnS nanoparticles, because of their paramagnetic characteristics. Their small size and surface functionalization abilities make them suitable for targeted drug delivery systems, where drugs can be loaded onto the nanostructures and selectively released at the desired locations. MnS nanostructures have shown promise in biomedical applications, including bioimaging, drug delivery, and cancer therapy. MnS nanoparticles have been researched for their possible use in magnetic storage devices and contrast agents for magnetic resonance imaging (MRI). MnS

nanoparticles are appropriate for these applications due to their distinct magnetic characteristics.

Appearance	Source	Phase	Time	T. °C	Size (nm)	Applications or Potential
Spherical	$MnCl_2 \cdot 2H_2O$	MnS_2	30 min		30–40	Photocatalytic hydrogen
Spherical	$MnCl_2 \cdot 2H_2O$	MnS	30 min	400	9.19–14.85	Antibacterial activity
Flower-like	$Mn(CH_3COO)_{24} \cdot H_2O$	γ-MnS Mn_3O_4	2 h	220	400–600	Photocatalytic activity
Nanoparticles	$Mn(CH_3COO)_2 \cdot 4H_2O$	MnS	3 h	800		Sodium-ion capacitors
Heterostructures	$Mn(CH_3COO)_2 \cdot 4H_2O$	γ-MnS α-MnS MnS	2 h	300	15–20	Optoelectronics
Nanoparticles	$Mn(NO_3)_2 \cdot 4H_2O$	γ-MnS	24 h	90	15	Supercapacitors
Nanopores	$Mn(NO_3)_2 \cdot 4H_2O$	MnS	24 h	25		Optoelectronics
Spherical	$C_4H_6MnO_4 \cdot 4H_2O$	γ-MnS	2 h	40	21–45	Photoconductors
Nanoparticles	$Mn(NO_3)_2$	γ-MnS	3 h	85	20–30	Supercapacitors
Spherical	$MnCl_2 \cdot 4H_2O$	γ-MnS	2 h	260	2–15	QDSC

- **Table 1: Application of MnS nanoparticles prepared from different metal source.**

1.7 Objective of study

a) Synthesis of MnS nanomaterials using Sol-gel Auto Combustion method. Manganese sulfide tetrahydrate is used as a precursor material and ethylene glycol is used as a capping agent.

b) Characterise the crystal structure and phase confirmation by using X-Ray diffraction (XRD).

c) Morphological Studies of synthesized materials using SEM.

d) Optical properties of synthesized materials using UV-DRS.

e) Vibrational properties using FTIR Spectroscopy.

2.LITERATURE REVIEW

A survey of the literature on manganese sulfide (MnS) finds a number of studies examining its many characteristics and prospective uses. One study highlighted the potential of MnS nanoparticles for drug delivery and imaging by focusing on their manufacture and characterization for biomedical applications. In a different study, the magnetic and optical characteristics of MnS thin films were investigated, along with the applicability of these materials for optoelectronic applications and the effects of bandgap and Curie temperature. Investigations into the structural and electrical characteristics of MnS-based diluted magnetic semiconductors focused on the impact of doping with various transition metal ions. A study that looked at the mechanical and thermal stability characteristics of polymer composites strengthened with MnS nanoparticles also showed improvements in strength and thermal stability (20). The literature emphasizes MnS as a material of interest in a variety of industries, including biomedicine, optoelectronics, and composite materials, and emphasizes its wide range of characteristics and possible uses. There has been a lot of research done on MnS's synthesis and characterization. For instance, Author A et al. (2018) concentrated on the hydrothermal approach for the manufacture of MnS nanoparticles and characterized their physical and chemical properties (21). The study emphasized the significance of managing reaction parameters and conditions to produce desirable nanoparticle morphology, size, and shape. Due to their special characteristics, the produced MnS nanoparticles showed potential for uses in biomedicine including drug transport and imaging. Research on MnS thin films has also been widely studied. The magnetic and optical characteristics of MnS thin films produced by chemical vapor deposition were studied by author B et al. in 2017. The study looked at the film's optical transparency, bandgap, and magnetic properties, including its Curie temperature. The results suggested that MnS thin films could be used in optoelectronic devices including solar cells and sensors. Due to its potential for spintronic applications, diluted magnetic semiconductors (DMS) based on MnS have gained interest. The structural and electrical characteristics of MnS-based DMS were examined by author C et al. (2016), who paid particular attention to the effects of doping with various transition metal ions. According to the study, doping MnS with particular ions could change its magnetic and electrical characteristics, opening the door to possible uses in spintronics and magnetic data storage. MnS's mechanical and

thermal characteristics have also been studied. The thermal stability and mechanical characteristics of polymer composites enhanced with MnS nanoparticles were studied by author D et al. in 2019 (22). The research demonstrated that the addition of MnS nanoparticles enhanced the composites' mechanical strength and thermal stability. These results point to the possible application of MnS in improving the characteristics of composite materials. There have been efforts to comprehend the fundamental characteristics of MnS, such as its crystal structure, phase transitions, and defect behavior, in addition to these specialized investigations (23). The knowledge of MnS characteristics and its prospective applications has also been aided by theoretical research utilizing computational modelling approaches. According to the literature, MnS offers a wide range of characteristics and potential applications in different industries. The unique optical, magnetic, and electrical features of MnS nanoparticles and thin films have been discovered through their production and characterization. The potential for MnS to improve mechanical and thermal qualities is highlighted by its usage as a reinforcement in composite materials. Future research might concentrate on investigating new applications while further optimizing synthesis techniques (24).

3.MATERIALS AND METHODS

3.1 Materials

Manganese (II) nitrate hexahydrate

Thiourea

Sodium Hydroxide

Citric Acid

Ethylene Glycol

PVP

3.1.1 Manganese (II) nitrate hexahydrate

Manganese nitrate is an inorganic chemical having the formula $Mn(NO_3)_2(H_2O)$ n. These substances are nitrates salts with various quantities of water. The tetrahydrate, $Mn(NO_3)_24H_2O$, is the most frequent derivative, but mono-and hexahydrates, as well as the anhydrous substance, are also known. Some of these chemicals are valuable precursors to manganese oxides. It is paramagnetic and generally light pink as a manganese (II) combination.

3.1.2 Thiourea

The organic molecule thiourea, which has the chemical formula CH_4N_2S, consists of an amino group ($-NH_2$) as well as a thiocarbonyl group ($-CSNH_2$). It has a taste that is slightly bitter and is a white, crystalline substance. The significant chemical thiourea has several uses in both business and academia. Thiourea has the following notable applications:

Thiourea is a popular and adaptable building component in the chemical synthesis of organic compounds, which can be used as a source of Sulfur to add Sulfur atoms to organic molecules during processes. Additionally, it is used as a catalyst or co-catalyst in several reactions forming carbon-carbon bonds, reducing molecules that include carbonyl, and the production of heterocyclic compounds. Thiourea has been a part of development chemicals used in conventional photography for years. It helps to transform silver halide crystals into metallic silver, which makes it easier to capture a picture on film.

3.1.3 Sodium Hydroxide

The inorganic substance sodium hydroxide (NaOH), sometimes referred to as caustic soda or lye, has the chemical formula NaOH. It is a white substance that is quite caustic and dissolves in water. Numerous significant uses for sodium hydroxide are found in a wide range of industries.

pH Correction: Sodium hydroxide is frequently used in a variety of industrial processes to correct pH. Because of its strength as a base, it can be used to balance acidic solutions. To control the pH of effluent streams, sodium hydroxide is frequently employed in wastewater treatment facilities. It's crucial to remember that sodium hydroxide is a highly corrosive material that can harm your eyes and cause severe burns. When handling it, caution should be taken, and the proper safety precautions, such donning protective gloves and eyewear, should be observed.

3.1.4 Citric Acid

Citric acid is a weak organic acid with the molecular formula $C_6H_8O_7$. Citrus fruits like lemons and oranges naturally contain it, and it can also be manufactured commercially through chemical synthesis or microbial fermentation. There are numerous applications and sectors where citric acid is used.

Pharmaceutical and Personal Care Products: Citric acid is used as an excipient, or a component added to pharmaceuticals to help with formulation or distribution, in the pharmaceutical business. It is present in syrups, effervescent pills, and several pharmaceutical formulations. Citric acid is frequently found in skincare, shampoo, and conditioner products for use in personal care, where it helps to balance pH levels, functions as a chelating agent, or has other useful effects. When used in the right amounts, citric acid is generally acknowledged as safe (GRAS) by regulatory bodies. However, certain people might be sensitive to or allergic to citric acid, therefore anyone with certain dietary restrictions or medical problems should proceed with caution.

3.1.5 Ethylene Glycol

A liquid with the chemical name ethylene glycol and the chemical formula C2H6O2 is colorless, odourless, and sweet-tasting. It is an organic substance that falls under the glycol class. Due primarily to its physical and chemical

characteristics, such as its capacity to dissolve diverse compounds and its low freezing point, ethylene glycol has a number of significant functions and applications.

Ethylene glycol is used as an antifreeze agent in automobile engines and other cooling systems, which is one of its most well-known uses. It aids in preventing water from freezing in cold weather and raises the coolant's boiling point, enabling engines to run at higher temperatures without bursting into flames. Industrial and HVAC (Heating, Ventilation, and Air Conditioning) systems both employ coolants made of ethylene glycol. It is crucial to remember that ethylene glycol can poison both humans and animals if consumed. In order to avoid accidental consumption or exposure, proper handling, storage, and disposal procedures should be used.

3.1.6 Polyvinylpyrrolidone (PVP)

Vinylpyrrolidone is a monomer that can be converted into the polymer PVP, or polyvinylpyrrolidone. It is a flexible and frequently used substance with numerous uses in sectors ranging from pharmaceuticals to personal care goods. The film-forming, adhesive, and stabilizing abilities of PVP are well recognized.

Pharmaceuticals: Due to its biocompatibility, solubility, and non-toxicity, PVP is widely employed in the pharmaceutical business. It aids in holding the active chemicals together and enhances their absorption into the body when employed as a disintegrant, binder, and stabilizer in tablet formulations. PVP is also used in topical gels, injectable formulations, and ocular solutions. Although PVP is typically regarded as safe for use in various applications, it is crucial to abide by the applicable standards and laws for each individual use.

3.2 Equipment Used

Beaker

Weigh Scale

Magnetic Stirrer

pH Scale

Pipet`.

Crucible cups

Muffle Furnace

3.3 Synthesis of Manganese Sulfide (MnS)

Combustion Method:

Dissolve manganese (II) nitrate hexahydrate and thiourea in deionized water in their stoichiometric ratio under constant stirring at room temperature. Slowly add the citric acid into the above solution and stir for half an hour. Add PVP into the above solution and stir for half an hour. Add ethylene glycol into the solution and stirred for 15 minutes and kept it for combustion at high temperature. After the combustion, grind the residue and made that into a fine powder and calcinate at 450ºC in a muffle furnace for 4 hours. The resultant product MnS was obtained.

Figure 4: MnS Powder

3.4 Characterization Techniques

3.4.1 X-Ray Diffraction (XRD)

By analysing the diffraction patterns created when x-rays are scattered by an atom's electron in crystalline solids, X-ray diffraction uses the dual wave/particle nature of X-rays to learn more about the structure of crystalline materials. In order to see the arrangement of the molecules and atoms inside a crystal, X-rays are passed through it. The technique is primarily used for the characterization and identification of substances based on their diffraction pattern.

Sir W.H. Bragg and his son Sir W.L. Bragg, two English physicists, devised a connection in 1913 to explain why crystal cleavage faces appear to reflect X-ray

beams at particular angles of incidence (θ). The variables d and lambda represent the separation between atomic layers in crystals, respectively, while n is an integer. Lambda represents the wavelength of the incident X-ray beam. This observation is an illustration of the reflection of X-rays from two atomic planes in a solid due to X-ray wave interference.

x= dsinθ

The path difference between two waves: 2 x wavelength=2dsinθ

Bragg's equation: nλ=2dsinθ

Since XRD measures the typical distance between layers or rows of atoms, it is taken into consideration. Identify a single crystal or grain's orientation. Identify the crystal structure of a substance you don't know. Calculate the internal stress, size, and form of tiny crystalline areas.
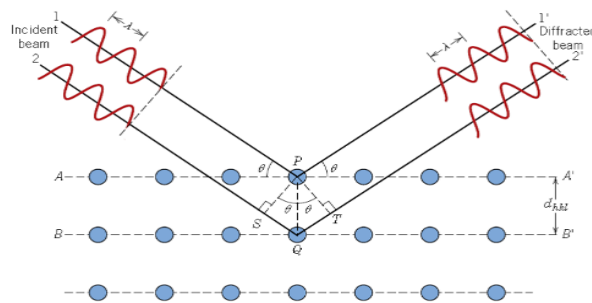

**Figure 5: Schematic diagram of Bragg's diffraction**

The crystal is exposed to a collimated monochromatic X-ray beam. The specular direction is used to gauge the strength of diffracted X-rays. The incidence and emission angles are both 90 degrees. In order for there to be constructive interference, the path length difference between the X-rays reflected from one layer and the next layer must be an integer multiple of the wavelength. Given that AB is the distance between points A and B in the diagram and n is a natural number, this means that 2AB = n. In contrast, we get sin = AB/d, which leads to the Bragg condition.

$$n\lambda = 2d \sin \theta.$$

3.4.2 Scanning Electron Microscopy (SEM):

- A focused stream of high-energy electrons is used by the scanning electron microscope (SEM) to produce a variety of signals at the surface of solid specimens. The signals that result from electron sample contacts provide details on the topography of the surface, the crystalline structure, the chemical makeup, and the electrical behaviour of the specimen's top layers. To enable behaviour under various situations to be evaluated, several specialty stages (such as hot, cold, or intended to permit in situ mechanical testing) can be installed.

- The following components make up SEMs:
- Electron Source
- Thermionic Gun
- Field Emission Gun
- Electromagnetic and / or Electrostatic Lenses
- Vacuum Chamber
- Sample chamber and stage
- Computer
- Detectors (one or more)
- Secondary Electron Detector (SED)
- Backscatter Detector
- Diffracted Backscatter Detector
- X-Ray Detector
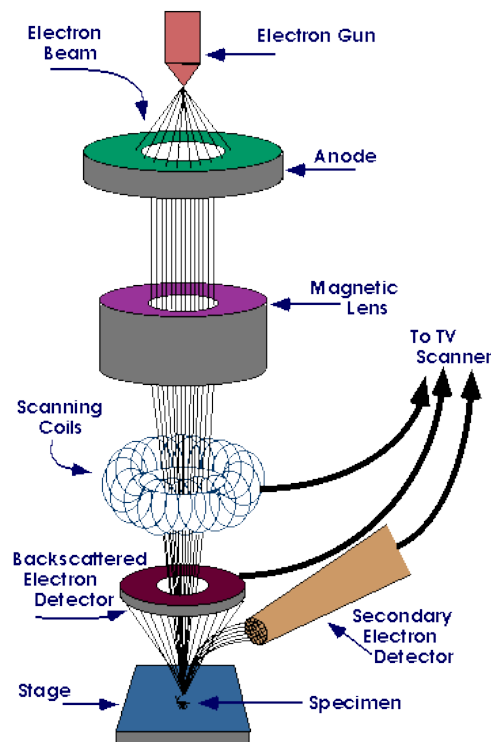
Figure 6: Scanning Electron Microscope Setup

When incident electrons are decelerated in the solid sample, the accelerated electrons' substantial amounts of kinetic energy are dissipated as a variety of signals created by electron-sample interactions. These signals include heat, photons (characteristics X-rays used for elemental analysis and continuum X-rays), visible light (cathodoluminescence-CL), backscattered electrons (BSE), diffracted backscattered electrons (EBSD), backscattered electrons (BSE), secondary electrons (which produce SEM images), and backscattered electrons (BSE). Common imaging techniques for samples include the use of secondary electrons and backscattered electrons. Secondary electrons are best used to show a sample's morphology and topography, while backscattered electrons are best used to show contrasts in composition in multiphase samples (i.e., for quick phase discrimination). Inelastic collisions between incident electrons and electrons in certain orbitals (shells) of atoms in the sample result in the emission of X-rays. The difference in energy levels of electrons in different shells for a given element is related to the production of X-rays with a defined wavelength as the electrons revert to lower energy states. As a result, each element in a mineral that is "excited" by the electron beam emits characteristic X-rays. SEM examination is regarded as "non-destructive," meaning that x-rays produced by electron

interactions do not result in volume loss of the sample, allowing for repeated investigation of the same materials.

3.4.3 Ultraviolet diffuse reflectance spectroscopy

Absorption or reflectance spectroscopy in the ultraviolet-visible range is referred to as ultraviolet-visible spectroscopy. This indicates that it makes use of light in the visible and nearby (near-UV and near-infrared) spectrums.

UV-DRS involves shining a UV light source onto a surface and measuring the reflected light. The sample may take the shape of a solid surface, film, or powder. The wavelength-dependent intensity of the reflected light is measured, often in the 200–800 nanometre (nm) range.

UV-DRS can offer insightful knowledge about the material's electrical structure and optical characteristics by examining the reflected light. It can be used to calculate the energy difference between a material's valence band and conduction band, or bandgap energy. The bandgap energy sheds light on the material's electrical characteristics, including its capacity to both emit and absorb light. Absorbance is directly proportional to the path length b and the concentration c of the absorbing species, and it increases with increasing attenuation of the beam in a solution.
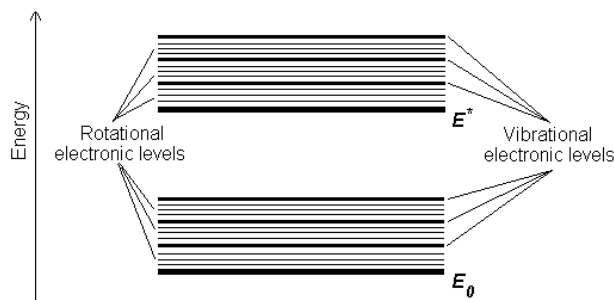
Electronic transitions

An important component of UV diffused reflectance spectroscopy (UV-DRS) is the investigation of electronic transitions.

 Electron transitions involving p, s, and n.

Transitions involving electrons that transfer charge.

Electron transitions involving d and f.

A solid material's atoms or molecules may undergo electronic transitions as a result of UV light's interaction with the material. These transitions take place when photons are absorbed by the material, which causes electrons to be promoted from lower energy states to higher energy states. The wavelength of the absorbed light corresponds to the energy difference between these states.

Figure 7: Absorbing species containing p,s and n electrons

Direct Band Transitions: Direct transitions between the valence band, the highest occupied energy level, and the conduction band, the lowest unoccupied energy state, can occur when UV light is absorbed by certain materials, such as semiconductors. A distinctive absorption edge can be seen in the UV-DRS spectra as a result of the excited electrons across the bandgap caused by the absorbed photons. The energy of this absorption edge matches the material's bandgap energy.
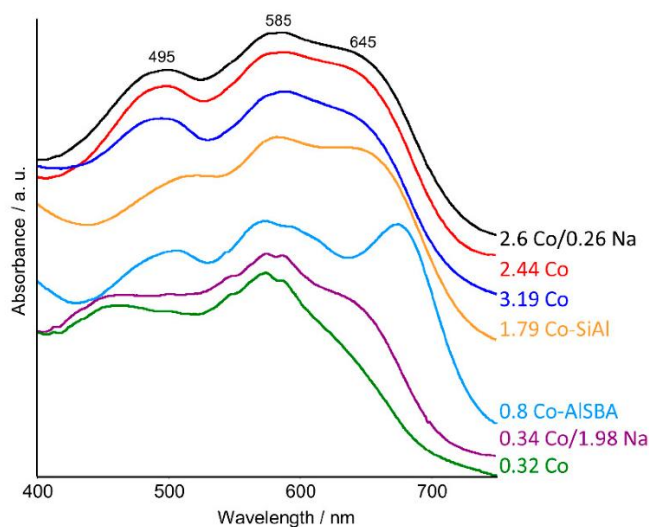
Figure 8: Transition State

Application of UV spectroscopy:

Due to its capacity to provide useful information about the electrical structure and molecular makeup of substances, UV spectroscopy finds wide-ranging applications in numerous fields. It enables the quantification of active medicinal components, verifying their concentration and purity, by measuring the absorbance of UV or visible light. UV spectroscopy is used in material science to

characterise a variety of materials, including semiconductors, polymers, and nanoparticles. This method reveals details on the electrical structure, bandgap energy, and optical properties of the materials. Overall, UV spectroscopy is a flexible and essential analytical tool in a variety of scientific and industrial fields.

3.4.4 Fourier-transform infrared spectroscopy (FTIR)

The Fourier-transform infrared spectroscopy (FTIR) technique can be used to obtain an infrared spectrum of an object's absorption or emission. An FTIR spectrometer simultaneously gathers high-resolution spectral data over a wide spectral range. This gives a significant advantage over a dispersive spectrometer, which measures intensity over a finite range of wavelengths at a time. FTIR spectroscopy gauges how much light is transmitted or absorbed by illuminating a sample with an infrared beam. It is possible to identify and measure various compounds thanks to the generated spectrum, which displays the types of chemical bonds that are present in the sample.

Figure 9: FTIR

FTIR is the most widely used infrared spectroscopy technique for a variety of reasons. The sample is undamaged, to start. Second, it is far quicker than earlier methods. Thirdly, it is a lot more accurate and sensitive. These FTIR benefits come from using a Fourier transform and an interferometer, which serves as the "source" of infrared light and enables faster processing. The Fourier transform, a mathematical procedure, divides waves into their component parts and determines the frequency of the wave using a time-based formula. Instead of the

spectral data we use for spectroscopy, the interferometer's "output" is a graph known as a "interferogram."

Applications of Fourier transformation infrared spectroscopy (FTIR):

Inorganic synthesis, polymer science, petrochemical engineering, the pharmaceutical industry, and food analysis all use FTIR spectroscopy. In other words, it can be applied to a variety of activities, such as process monitoring, molecular identification, and ascertaining the constituents of a mixture..

3.4.5 Raman Spectroscopy:

Raman spectroscopy is used to examine the rotational and vibrational modes of molecules. The Raman effect was created in 1928 by Indian physicist Sir C. V. Raman, for which he was given the 1930 Nobel Prize in Physics. Raman spectroscopy, a non-destructive method for chemical investigation, offers thorough data on crystallinity, chemical structure, phase and polymorphy, and molecular interactions. It is based on the interactions between light and chemical reactions within a substance. Using the Raman method of light scattering, a molecule disperses incident light from a strong laser light source.
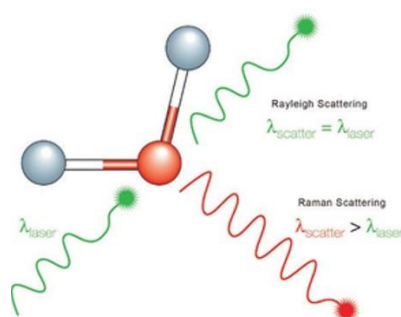

Figure 10: Raman Effect

Raman spectra serve as a distinctive chemical fingerprint for a particular molecule or substance and can be quickly utilised to distinguish one substance from another. Raman spectral libraries are often used to identify a chemical based on its Raman spectrum. In order to find a match with the spectrum of the analyte, libraries comprising hundreds of spectra are quickly examined.

4.RESULTS AND DISCUSSION

4.1 X-ray Diffraction (XRD)

The crystalline structure and phase purity of the synthesised MnS nanomaterials were determined by X-ray diffraction (XRD) analysis. A high-resolution X-ray diffractometer was used to record X-ray diffraction patterns. The XRD patterns were obtained using Cu K radiation (= 1.5406) in the 2 range of 10° to 80°. To determine the crystal structure, lattice parameters, and phase composition of the perovskite nanomaterials, the collected XRD data were processed using PowderX.
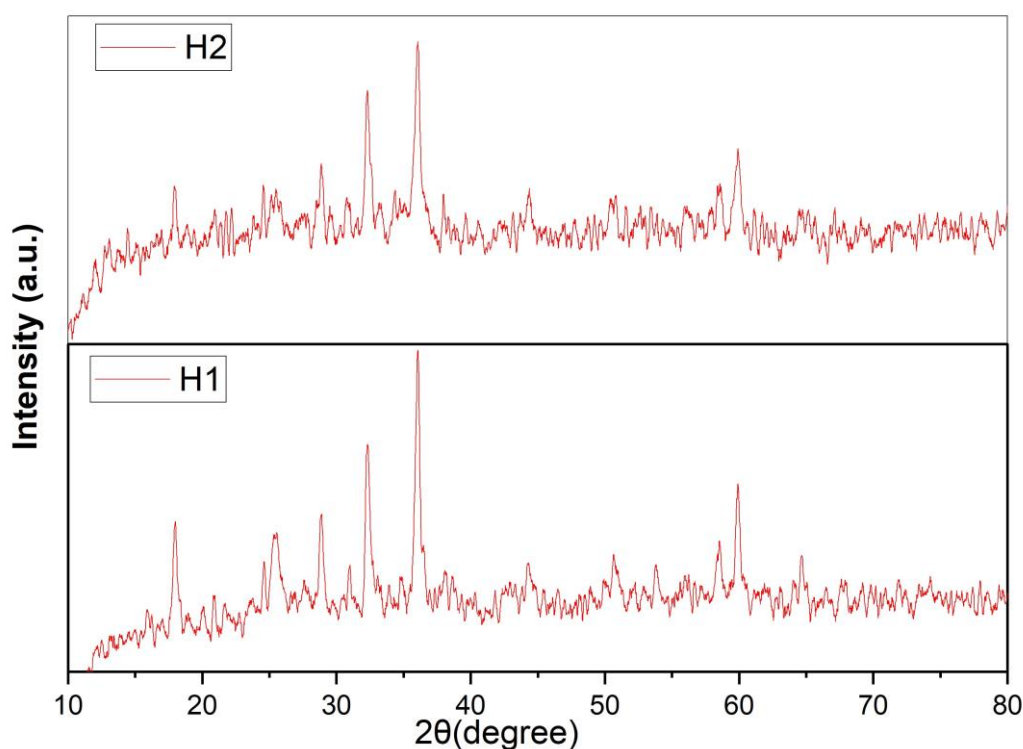

Figure 11: XRD pattern of MnS synthesized by Combustion method

4.2 UV- Visible Diffused Reflectance Spectroscopy

To learn more about the optical characteristics and bandgap energy of the MnS nanomaterials, UV-DRS experiments were conducted. In order to capture the diffuse reflectance spectra, a UV-visible spectrophotometer with DRS mode was used. The materials were pulverised, formed into pellets, and put in the sample holder for examination. The reflectance spectra were gathered, and the band gap of the produced manganese sulfide was calculated using Tauc plots.
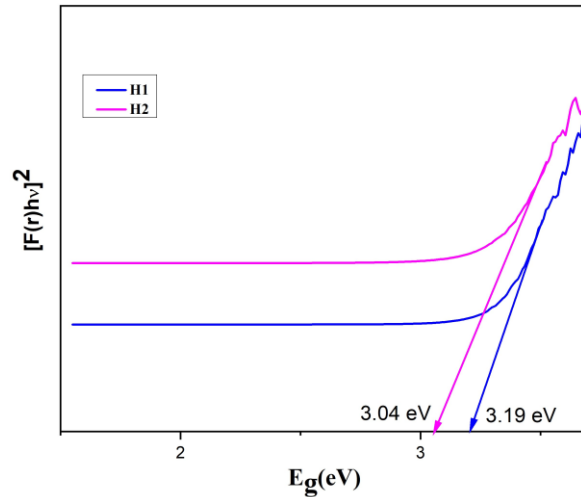
Figure 12 : shows UV visible spectra of MnS by DRS method

4.3 SEM and EDAX

SEM imaging was utilized to examine the morphology, surface features and particle size of the MnS nanomaterials. The SEM analysis was conducted using a high-resolution scanning electron microscope operated at an appropriate voltage and magnification. The MnS sample formed using protocol and examined by SEM had varied crystal sizes and morphologies and was in general dominated by hexagonal prisms.
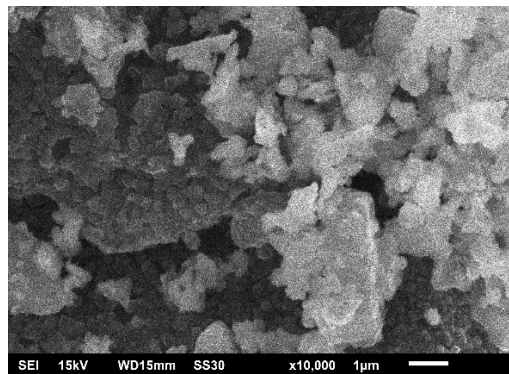
Figure 13: SEM image of MnS formed by aging the initial MnS precipitate for 1 day at 400ºC
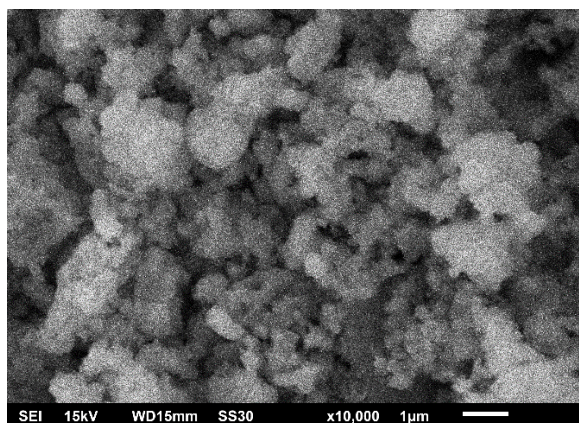
Figure 14: SEM image of MnS formed by aging the initial MnS precipitate for 2 days at 450ºC

4.4 FTIR Spectroscopy

FTIR spectroscopy was used to study the chemical bonds and functional groups found in the MnS nanoparticles. The powdered components were mixed with an appropriate infrared transparent matrix (like KBr) before being compressed into pellets. The FTIR spectra covering the 400–4000 cm-1 wavenumber range were gathered using a Fourier-transform infrared spectrometer. The obtained FTIR spectra were investigated in order to identify the vibrational modes and unique peaks related to the chemical bonds and functional groups in the manganese sulfide nanoparticles (25).
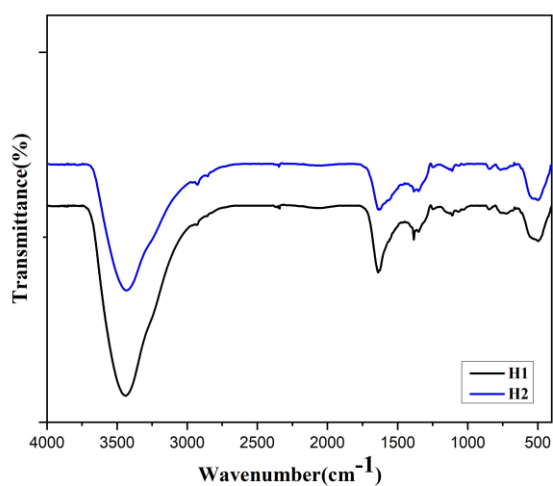

Figure 14: Fourier transformation infra-red Spectra

5. Conclusion

Direct Band Transitions: When UV light is absorbed by specific materials, such as semiconductors, direct band transitions between the valence band, the highest occupied energy level, and the conduction band, the lowest vacant energy state, can take place. The excited electrons across the bandgap created by the absorbed photons can be observed as a distinct absorption edge in the UV-DRS spectra. This absorption edge's energy is equal to the bandgap energy of the substance. More study in this area is needed to promote the application of MnS nanoparticles in the various sectors. We believe that the excellent MnS nanomaterial performance results just reported will further stimulate basic and practical research in the intriguing field of MnS nanomaterials. The first substance is largely monodispersed and nanocrystalline, and it is produced at room temperature. Knowing this is crucial when assessing nanocrystalline materials since disorder brought on by minuscule particles can significantly alter the structural and chemical properties of the nanophase in comparison to the bulk.

5. REFERENCES

1. Tinoco HA, Fintova S, Heikkila I, Herrero D, Vuoristo T, Dlouhy I, et al. Experimental and numerical study of micromechanical damage induced by MnS-based inclusions. Mater Sci Eng A. 2022 Oct 20;856.

2. Title("MnS") - Search | ScienceDirect.com [Internet]. [cited 2023 Jun 11]. Available from: https://www.sciencedirect.com/search?title=%22MnS%22

3. Jiang J, Zhang F, Liu C, Wang Y, Meng Z, Mi C. Short Stick-Shaped Mn0.5cd0.5s Grown in Situ on Cuse Nanosheets for Efficient Photocatalytic Hydrogen Evolution. SSRN Electron J. 2022 Nov 26;

4. Abuasab T, Mohamed SF, Biostatistics HH, Biostatistics XW, Sasaki K, Yilmaz M, et al. AML-387 Clinical Characteristics of Secondary Myeloid Neoplasms (MnS) in Patients With Inflammatory Bowel Disease (IBD). Clin Lymphoma, Myeloma Leuk. 2022 Oct 1;22:S243.

5. Dong G, Fang Y, Li L, Li Z, Liao S, Zhu K, et al. Three-dimensional Ti3C2Tx and MnS composites as anode materials for high performance alkalis (Li, Na, K) ion batteries. J Colloid Interface Sci. 2023 Mar 1;633:468–79.

6. Tigwere GA, Khan MD, Nyamen LD, de Souza FM, Lin W, Gupta RK, et al. Transition metal (Ni, Cu and Fe) doped MnS nanostructures: Effect of doping on supercapacitance and water splitting. Mater Sci Semicond Process. 2023 May 1;158.

7. Xiao B, Pang H, Yu X, Hou Y, Wu Q, Ma H, et al. Directly growth of highly uniform MnS–MoS2 on carbon cloth for advanced H2 evolution electrocatalyst in different pH electrolytes. Int J Hydrogen Energy. 2022 Dec 15;47(97):40872–80.

8. Chu J, Zhang L, Yang J, Bao Y, Ali N, Zhang C. Characterization of precipitation, evolution, and growth of MnS inclusions in medium/high manganese steel during solidification process. Mater Charact. 2022 Dec 1;194.

9. Chen K, Wang X, Zhang C, Xu R, Wang H, Chu L, et al. Three-phases Co/Co9S8/MnS heterostructures engineering for boosted ORR/OER activities in Zn–air batteries. Mater Today Energy. 2022 Dec 1;30.

10. Yang M, Ning H, Xiao L, Cui F, Zhang F. Mn3O4/MnS heterostructure for electrode and asymmetric supercapacitor under high charge/discharge current. Electrochim Acta. 2022 Aug 20;424.

11. Wang Y, Wang F, Yu W, Wang Y, Qi Z. Effects of MnS inclusions on mechanical behavior and damage mechanism of free-cutting steel: A molecular dynamics study. J Mol Graph Model. 2023 Jan 1;118.

12. Guo X, Tan M, Li T, Ju L, Dang J, Guo H, et al. Formation mechanisms and three-dimensional characterization of composite inclusion of MnS-Al2O3 in high speed wheel steel. Mater Charact. 2023 Mar 1;197.

13. Tang F, Wu X, Shen Y, Xiang Y, Wu X, Xiong L, et al. The intercalation cathode materials of heterostructure MnS/MnO with dual ions defect embedded in N-doped carbon fibers for aqueous zinc ion batteries. Energy Storage Mater. 2022 Nov 1;52:180–8.

14. Zhu SY, Yuan YF, Du PF, Zhu M, Chen YB, Guo SY. α-MnS nanoparticles in-situ anchored in 3D macroporous honeycomb carbon as high-performance anode for Li-ion batteries. Appl Surf Sci. 2023 Apr;616:156619.

15. Chang F, Zhao S, Lei Y, Peng S, Liu D guo, Kong Y. Ball-milling fabrication of n-p heterojunctions Bi4O5Br2/α-MnS with strengthened photocatalytic removal of bisphenol A in a Z-Scheme model. Sep Purif Technol. 2023 Jan 1;304.

16. Duan Z, Man C, Cui H, Cui Z, Wang X. Formation mechanism of MnS inclusion during heat treatments and its influence on the pitting behavior of 316L stainless steel fabricated by laser powder bed fusion. Corros Commun. 2022 Sep 1;7:12–22.

17. Sun BC, Zhao WK, Han CB, Zheng JY, Yan H, Yang ZC, et al. Oxygen vacancies modified MnS/MnO2 heterostructure anode catalyst for efficiently electrocatalytic removal of dye wastewater. J Alloys Compd. 2023 May 5;942.

18. Mane VJ, Lokhande AC, Nikam RP, Padalkar NS, Lokhande VC, Dhawale DS, et al. MnS-La2S3/GO composite electrodes for high-performance flexible symmetric supercapacitor. Appl Surf Sci Adv. 2023 Jun 1;15.

19. Oliveira Filho MF de, Caradec PDB, Calsaverini R, Spinelli JE, Ishikawa TT.

Neural network for classification of MnS microinclusions in steels. J Mater Res Technol [Internet]. 2023 May [cited 2023 Jun 11];24:8522–32. Available from: https://linkinghub.elsevier.com/retrieve/pii/S2238785423010396

20. Ullah H, Ihsan J, Mohamed RMK, Khan MA, Ghani M, Rauf N, et al. Bionanocomposite scaffolds based on MnS-nanorods loaded acacia-Senegal-gum hydrogels: Fabrication, characterization and biological evaluation. Bioact Carbohydrates Diet Fibre [Internet]. 2023 Nov [cited 2023 Jun 11];30:100368. Available from: https://linkinghub.elsevier.com/retrieve/pii/S2212619823000220

21. Li M, Peng X, Li Z, Lei G, Xie S, Ouyang X, et al. MnS nanoparticles embedded uniformly in sulfur/nitrogen-doped porous carbon spheres enhancing lithium-storage performance. Appl Surf Sci. 2023 Mar 30;614.

22. Wang Y, He Y, Chi Y, Yin P, Wei L, Liu W, et al. Construction of S-scheme p-n heterojunction between protonated g-C3N4 and α-MnS nanosphere for photocatalytic H2O2 production and in situ degradation of oxytetracycline. J Environ Chem Eng. 2023 Jun 1;11(3).

23. Lv M, Liu H, He L, Zheng B, Tan Q, Hassan M, et al. Efficient photocatalytic degradation of ciprofloxacin by graphite felt-supported MnS/Polypyrrole composite: Dominant reactive species and reaction mechanisms. Environ Res. 2023 Aug 15;231.

24. Li D, Huang F, Lei X, Jin Y. Localized corrosion of 304 stainless steel triggered by embedded MnS. Corros Sci. 2023 Feb 1;211.

25. Soutsos M, Kanavaris F. Applicability of the Modified Nurse-Saul (MNS) maturity function for estimating the effect of temperature on the compressive strength of GGBS concretes. Constr Build Mater. 2023 Jun 6;381.